Efficiency of Permanent Magnet Synchronous Motors for Various Current Vector Controls

著者	Tong Yi, Morimoto Shigeo, Takeda Yoji, Hirasa Takao
引用	Bulletin of University of Osaka Prefecture. Series A, Engineering and natural sciences. 1990, 39(1), p.29-37
URL	http://doi.org/10.24729/00008452

Efficiency of Permanent Magnet Synchronous Motors for Various Current Vector Controls

Yi TONG*, Shigeo MORIMOTO**, Yoji TAKEDA** & Takao HIRASA**

(Received June 16, 1990)

The steady-state performance of permanent magnet synchronous (**PM**) motors can be modelled by the *d-q* axis equivalent circuit, which include the effect of the stator copper loss and core loss. For constant torque or constant speed operation, the efficiency of the **PM** motor depends on the current vector control methods and the rotor geometry.

In this paper, the efficiency of the **PM** motor for various current vector control methods and the rotor geometries are examined. Under the inverter restrictions, flux-weakening control is very useful to extend the operating speed range. The efficiency of flux-weakening control is also examined.

1. Introduction

Permanent magnet synchronous motors are widely used in industrial applications such as machine tools, robotics, actuators and electric vehicles. The **PM** motor always operates at synchronous speed and therefore does not have slip losses inherently as induction motor drives. In addition, since the field excitation in the **PM** motor is provided by permanent magnets, the **PM** motor does not have a field winding loss.

Although the **PM** motor generally offers high efficiency and high power factor compared with an induction or conventional **DC** machine in adjustable-speed drives, the efficiency of the **PM** motor depends on the control methods and the rotor geometry. To perform the low cost operations of the **PM** motor driving system, the analysis and examination of the efficiency are important.

The **PM** motor have various geometries of the rotor. The **PM** motors can be classified according to the salient coefficient ρ, which is d- and q-axis inductance ratio ($\rho = L_q/L_d$). The typical rotor geometries are shown in Fig. 1. In the surface permanent magnet motor (Fig. 1 (a), (b)), magnets may be placed on the surface of

* Graduate Student, Department of Electrical Engineering, College of Engineering.

** Department of Electrical Engineering, College of Engineering.

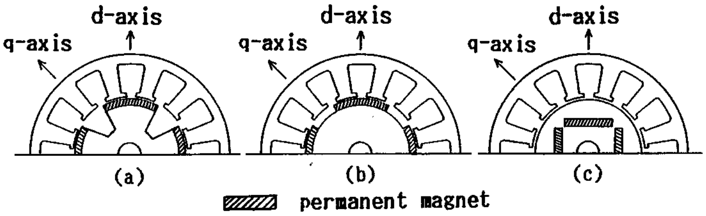

Fig. 1 Cross sections of PM motors. (a) Surface ($\rho<1$). (b) Surface ($\rho=1$), (c) Interior ($\rho>1$).

the rotor. In the interior permanent magnet motor (Fig. 1 (c)), magnets are buried within the rotor core. As a relative permeability of a permanent magnet is very nearly unity, the magnet space behaves like an air. Therefore, the **PM** motor shown in Fig. 1 (a) is a salient type machine ($\rho<1$), and the surface **PM** motor shown in Fig. 1(b) is a non-salient type machine ($\rho=1$). On the other hand, the interior **PM** motor is a contrary salient type machine ($\rho>1$).

The purpose of this paper is to examine the efficiency characteristics of the **PM** motor controlled by the various current vector control methods considering the saliency of the machine.

2. Basic Equations and Equivalent Models

For the steady state operation, Fig. 2 shows the equivalent circuits including saliency of the machine in the synchronously rotating reference frame, where all the parameters are given in the per-unit expression.[1] The basic equations of the **PM** motor are derived from above d-q equivalent circuits.

$$\begin{bmatrix} V_d \\ V_q \end{bmatrix} = R_a \begin{bmatrix} i_d \\ i_q \end{bmatrix} + \alpha \begin{bmatrix} V_{xd} \\ V_{xq} \end{bmatrix} \tag{1}$$

$$\begin{bmatrix} V_{xd} \\ V_{xq} \end{bmatrix} = \begin{bmatrix} 0 & -\omega\rho X_d \\ \omega X_d & 0 \end{bmatrix} \begin{bmatrix} i_d \\ i_q \end{bmatrix} + \begin{bmatrix} 0 \\ \omega E_o \end{bmatrix} \tag{2}$$

$$T = I_a \ \{E_o\cos\beta_o + \frac{1}{2}(\rho-1)X_d I_a \sin 2\beta_o\} \tag{3}$$

$$P = T\omega \qquad i_d = -I_a\sin\beta_o,\ i_q = I_a\cos\beta_o \tag{4}$$

where

ω : speed

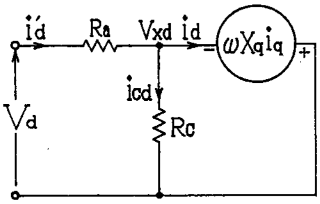

(a) d-axis equivalent circuit.

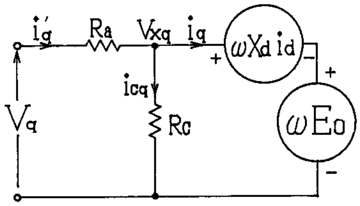

(b) q-axis equivalent circuit.

Fig. 2 Equivalent circuits of PM motor.

E_o : open circuit voltage at unity speed
X_d : direct axis reactance at unity speed
β_o : leading angle of armature current
R_a : stator winding resistance per phase
R_c : core loss resistance
$\alpha = 1 + R_a/R_c$: loss parameter
I_a : armature current per phase
V_d : direct axis component of armature voltage
V_q : quadrature axis component of armature voltage
T : output torque
P : output power

These equations will be presented in their per unit form with base values of voltage, current and speed chosen as the rated values.

In the torque Equation (3), the first term represents the magnet torque and the second term can be recognized as the reluctance toruque.

The major contributor to electrical losses in the **PM** motor derives from two sources. The one is the stator copper loss and the other is the core loss.

These losses are presented by the resistances in the *d-q* equivalent circuit shown in Fig. 2. The core loss in the machine is accounted by the shunt resistance R_c. The voltage V_x that appears across this resistance corresponds to the stator flux-linkage, which induces the core loss. The copper loss and the core loss as well as the efficiency can be expressed in terms of the equivalent-circuit parameters

$$W_{cu} = R_a(i_d + V_{xd}/R_c)^2 + R_a(i_q + V_{xq}/R_c)^2 \tag{5}$$

$$W_{Fe}=\frac{V_{xd}^2}{R_c}+\frac{V_{xq}^2}{R_c}=\frac{V_x^2}{R_c} \tag{6}$$

$$\eta=\frac{P}{P+W_{cu}+W_{Fe}}\times 100(\%) \tag{7}$$

3. Current Vector Controls and Effiiency

Figure 3. shows the scheme of the current phase control system. The system consists of a voltage source **PWM** inverter, rotor position sensor, current sensors, speed and current controllers. The current phase β_o is controlled according to the armature current command i^*. The relationship between β_o and i^* is decided by the various current phase control methods.

In practical control, the relationships between the input current magnitude and its phase β_o are necessary. Since the core loss current components i_{cd}, i_{cq} are very small, it is no problem that the core loss resistance can be neglected at this stage of control method derivation.

3.1. Current Phase Control Methods[2-4]

In this paper the following current phase control methods are examined.

(1) $i_d = 0$ control method

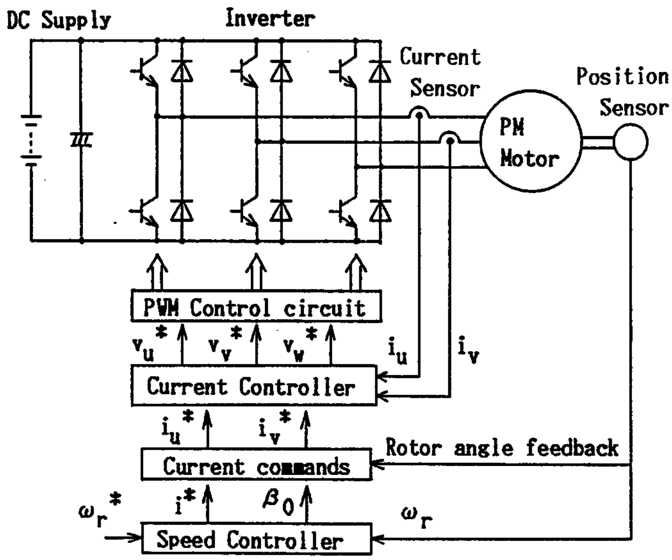

Fig. 3 Scheme of current phase control system.

Many **PM** motor drives are operated by this control method, where the direct axis component of the armature current is not exist. This control method is becoming of general use, because of its avoiding a demagnetizing action for the permanent magnet. The terminal voltage of the motor increases with load by the q-axis armature reaction.

(2) Constant flux-linkage control method
By controlling the current phase β_o according to the armature current, then the flux-linkage can be kept constant. The relationship between the armature current and its phase is given as follows by the condition of $V_x/(\omega\ E_o)=1.0$

$$\beta_o=\sin^{-1}\frac{E_o-\sqrt{E_o^2-(1-\rho^2)(\rho X_d I_a)^2}}{(1-\rho^2)X_d I_a} \tag{8}$$

(3) Maximum torque-per-Amp control method
Using the reluctance torque, the motor can be operated at the maximum attainable torque per stator current. The relation between the current magnitude I_a and its phase β_o can be obtained from $dT/d\beta_o=0$ and $d^2T/d\beta_o^2<0$.

$$\beta_o=\sin^{-1}\frac{-E_o+\sqrt{E_o^2+8(\rho-1)^2(X_d I_a)^2}}{4(\rho-1)X_d I_a} \tag{9}$$

3.2. Losses and Efficiency

To examine the efficiency of the above current phase control methods, there are two ways. The one is to change the torque at constant speed, the other is to change the speed at constant torque.

The parameter values in per units for two type **PM** motors such as the salient type and the contrary salient type machine are listed in table 1.

Figure 4 and Fig. 5 show the efficiency for the contrary salient **PM** motor ($\rho=3$) and the salient **PM** motor ($\rho=0.5$) at rated speed as a function of torque.

For the contrary salient **PM** motor, as shown in Fig. 4, the terminal current and voltage increase rapidly as load torque increases in the $i_d=0$ control method. Therefore, the copper loss and core loss become large. The operation of the constant flux-linkage control requires flux-weakening technique, which reduce the air gap flux by the negative d-axis current to hold the flux-linkage constant. This method requires excessive flux-weakening current, therefore greater copper loss yields than $i_d=0$ control method. The maximum torque-per-Amp control method minimizes the copper loss. This control method yields the higher efficiency at large torque operation than the other control methods.

The efficiency for the salient type **PM** motor ($\rho=0.5$) are shown in Fig. 5. As contrasted with the contrary salient type **PM** motor, the $i_d=0$ control method yields the high efficiency.

The core loss becomes dominant as the speed increases since the hysteresis loss is in proportion roughly to the input voltage frequency and the eddy current loss is in

Table 1 Parameters for simulation.

Parameter	Contrary salient	Salient
ρ	3.0	0.5
E_0	0.5	0.83
X_d	0.26	0.7
R_a	0.1	
R_c	15	

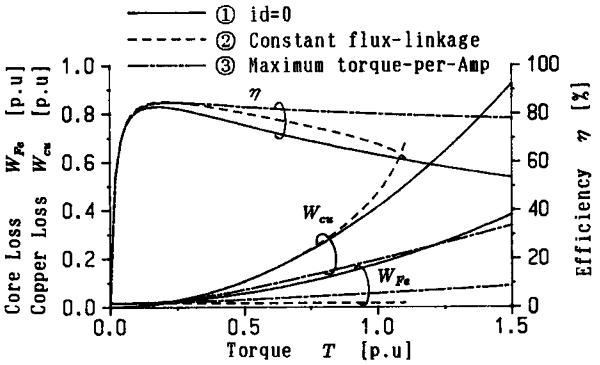

Fig. 4 Efficiency for contrary salient type PM motor at rated speed ($\rho=3.0$).

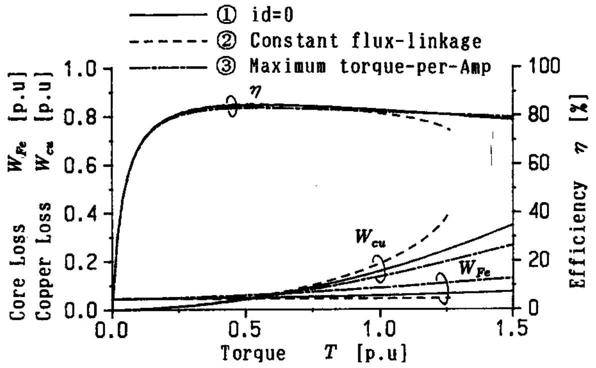

Fig. 5 Efficiency for salient type PM motor at rated speed ($\rho=0.5$).

proportion to frequency squared. To operate the *PM* motor at higher efficiency over a wide speed range, the field weakening is required at higher speeds to reduce the core loss.

Figure 6 illustrates the efficiency for the contrary salient type motor at the rated torque. The $i_d=0$ control method does not provide any field weakening effect, therefore the excessive core loss yields. The constant flux-linkage control method keeps the voltage V_x for constant so that this method offers a greater overspeed operation at high efficiency. At low speed, the core loss is less significant and a good

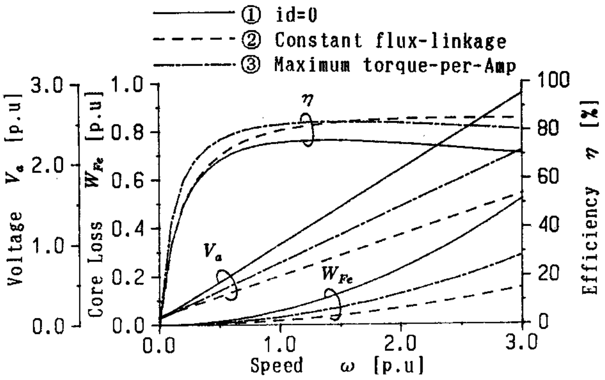

Fig. 6 Efficiency for contrary salient type PM motor at rated torque ($\rho=3.0$).

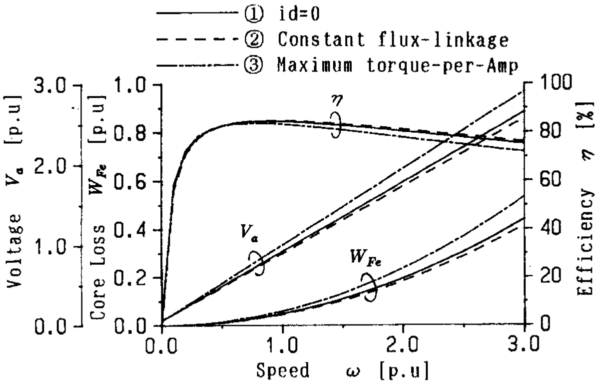

Fig. 7 Efficiency for salient type PM motor at rated torque ($\rho=0.5$).

operating method is the maximum torque-per-Amp control method. At higher speeds, this method does not provide the large field weakening and allows somewhat more core loss than the constant flux-linkage method.

For the salient type *PM* motor, the constant flux-linkage control method has a very small i_d so that this control method nearly approximates the $i_d=0$ control method. The maximum torque-per-Amp control method has relatively lower efficiency, as the terminal voltage increases with the positive magnetization current.

4. Efficiency in Flux-weakening Operation

The motor reactance and **EMF** are all proportional to the excitation frequency. As the rotor speed increases, the motor terminal voltage approaches to the maximum voltage of the inverter and the output power decreases. Consequently, the inverter limitation must be taken into account at very high speed. In order to expand the operating speed range, the flux-weakening control is very useful, which use the

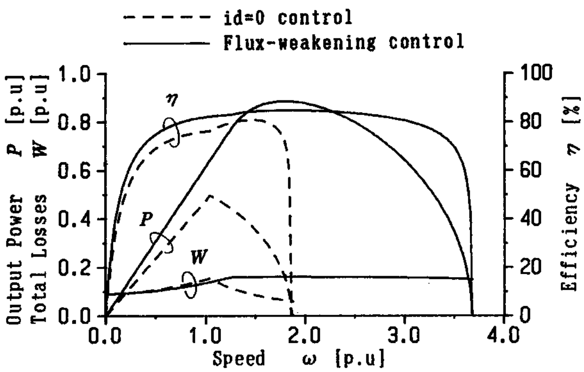

Fig. 8 Operating characteristics for $i_d=0$ control and flux-weakening control ($\rho=3.0$).

d-axis armature reaction to reduce the air gap flux.[5-8] The efficiency of flux-weakening control can be also examined using the equivalent circuits shown in Fig. 2.

Figure 8 shows the operating characteristics for the $i_d=0$ control and the flux-weakening control ($\rho=3.0$). As seen in Fig. 8, it is clear that the flux-weakening control keeps higher efficiency than the $i_d=0$ control. The flux-weakening control method significantly extends the operating speed range and improves the output power performance over the $i_d=0$ control method.

5. Conclusion

Using a simple model of the *PM* motor considering the copper loss and the core loss, the efficiency characteristic for various current vector control methods have been examined. These investigations provide some guidance in selecting the current vector control method for the contrary salient type and the salient type *PM* motor. From simulations, the following remarkable results are obtained.

(1) The control method to achieve the high efficiency must be selected according to the rotor geometry.

(2) For the contrary salient type **PM** motor, the constant flux-linkage control method is comparably well suited at high speed operation.

(3) For the salient type **PM** motor, the $i_d = 0$ and the constant flux-linkage control methods are desirable at high speeds.

(4) The maximum torque-per-Amp control method yields high efficiency especially at the large torque region and is more suited to applications where fast dynamic performance is required.

(5) The flux-weakening control achieves not only wide operating speed range but also the high efficiency.

References

1) R.S. Colby and D.W. Novotny, *IEEE Trans. Ind. Appl.,* vol. IA-23, no. 6, pp. 1048−1054, Nov./Dec. 1987
2) P. Viarouge, M.L. Mazenc, C. Andrieux, *IEEE Trans. Ind. Appl.,* vol. IA-23, no. 3, pp. 526−531, May/June, 1987
3) Y. Takeda, T. Hirasa, *PESC'88 Conf. Rec.,* pp. 409−414, 1988
4) S. Morimoto, Y. Takeda, T. Hirasa, *PCIM'88 Conf. Rec.,* pp. 77−86, 1988
5) B. Sneyers, D.W. Novotny, T.A. Lipo, *IEEE Trans. Ind. Appl.,* vol. IA-21, no. 2, pp. 398−407, Mar/Apr. 1985
6) T. Jahns, *IEEE Trans. Ind. Appl.,* vol. IA-23, no. 4, pp. 681−689, July/Aug. 1987
7) T. Sebastian, G.R. Slemon, *IEEE Trans. Ind. Appl.,* vol. IA-23, no. 6, pp. 327−333, Mar./Apr. 1987
8) S. Morimoto, Y. Takeda, T. Hirasa, K. Taniguchi, *IEEE-IAS Ann. Meeting, Conf. Rec.* pp. 51−56, 1989